

# BASIC DERIVATIVE DIAGNOSTICS

Jeffrey W. Knight  
Halliburton Energy Services

## ABSTRACT

Over the last decade the use of the pressure derivative as a diagnostic tool in pressure transient analysis has grown immensely. The modern well test analyst turns to the derivative log-log plot almost exclusively to formulate a first opinion on well test behavior. The pressure derivative essentially allows the analyst a magnified view of the distinctive pressure behavior associated with various wellbore and reservoir phenomena. This paper utilizes both real and simulated pressure transient data to illustrate common derivative responses due to selected wellbore and near-wellbore effects, reservoir types, and boundary conditions. Definitions of common well test analysis terminology are included. The information presented should allow individuals who are involved in well testing, but not necessarily confident in test analysis, to qualitatively comment on test results.

## INTRODUCTION

The advent of the pressure derivative, along with the introduction of high resolution electronic pressure recorders (which made the derivative approach feasible), have facilitated a revolutionary change for the better in well test interpretation. Described uses of pressure derivative appeared in the literature in the early 1980s for selected cases of interference tests<sup>1</sup>, two parallel faults<sup>2</sup>, and hydraulically fractured wells.<sup>3</sup> Three articles appearing in 1983-84 likely popularized the now widely accepted technology by extolling the merits of the derivative approach in the analysis of wells exhibiting wellbore storage and skin in infinite-acting homogeneous reservoirs<sup>4,5</sup> and in two-porosity reservoirs.<sup>5,6,7</sup> Today, no theoretical well test model is complete without the "picture" presented by the accompanying derivative. Certainly, no well test analyst, experienced or otherwise, would prefer to qualitatively comment on or quantitatively analyze well test data without benefit of the derivative.

Prior to the derivative log-log plot approach, the standard log-log plot was utilized in tandem with a semilog plot to attempt test diagnosis. The derivative log-log plot effectively combines the former two plots into one plot for diagnostic purposes. The derivative actually represents the change in slope of the test period data on the semilog plot. Therefore, the derivative merges the more sensitive semilog plot with the log-log plot, allowing a high resolution test picture to be seen from start to finish. This is significant because the log-log plot and older radial flow type curves<sup>8,9</sup> occasionally suffered from a lack of uniqueness. Furthermore, late-time test responses due to features such as boundaries produced little characteristic signature due to the small pressure changes at late-time and the compressional effect of the

log-log scale itself. The derivative allows better and more confident detection of early, middle and late-time test features. (Readers should see Ref. 10 for additional information on the use of pressure derivative.)

## **DEFINITIONS**

The following well test analysis terminology will be useful for the duration of the paper.

### **Linear Flow**

When the controlling reservoir fluid movement is one dimensional (Fig. 1), linear flow exists. Under certain conditions a linear profile may be seen on well test data where the well has been fractured; where the well is situated between two parallel boundaries; and where the well is horizontal.

### **Radial Flow**

When the controlling reservoir fluid movement converges to a point (the well) in any horizontal plane, but is linear through any vertical plane (Fig. 2), radial flow exists. Radial flow is the most common flow profile seen in practice.

### **Spherical Flow**

When the controlling reservoir fluid movement converges to a point (the well) in the horizontal and vertical planes (Fig. 3), spherical flow exists. A spherical flow profile is most likely seen on well test data where the well has only a small interval of the total net pay open to flow.

### **Early Time Region (ETR)<sup>12</sup>**

This region of the test data is commonly referred to as the wellbore storage and skin effects dominated data that occurs during the early portion of most well tests. Fluid movement within the wellbore and through the near-wellbore altered permeability region dominates the pressure response. Wellbore storage concerns unequal mass transfer due to fluid compressional or decompressional behavior, and/or rising or falling liquid levels. Wellbore storage effects mask the true reservoir pressure response and can totally obscure any near-wellbore, reservoir, or boundary effect described in this paper. The physical conception of skin is that of a near-wellbore region of altered permeability. Drilling and completion operations are prime sources of near-wellbore permeability reduction, and stimulation treatments are the prime source of near-wellbore permeability improvement.

The definition of ETR for purposes of this paper is extended to include all early, short term pressure responses due to physically imposed near-wellbore features such as hydraulic fractures,

horizontal wells, etc. This is consistent with methodologies of modern well test analysis software.

### **Middle Time Region (MTR)<sup>12</sup>**

After ETR effects cease to dominate the pressure response, the bulk or virgin formation controls the pressure response. The formation or reservoir model may be that of a homogeneous single porosity reservoir, a naturally-fractured (two-porosity) reservoir or possibly something else. During MTR the reservoir responds as if it were infinite in extent, i.e., no influence of boundaries, and the derivative assumes a constant value or flattens. The derivative flattening coincides with the data achieving a constant slope on the semilog analysis plot. These data represent the analyzable portion of the test via straight-line or semilog analysis where the semilog slope is inversely related to transmissibility ( $kh/\mu$ ). Infinite-acting radial flow or a near-radial flow profile (called pseudo-radial flow) controls the response during MTR.

### **Late Time Region (LTR)<sup>12</sup>**

As a well test progresses in time and a larger portion of the reservoir is sampled, no-flow boundaries, constant pressure sources, and changes in formation thickness ( $h$ ) or fluid mobility ( $k/\mu$ ) can influence the pressure response. Once the pressure response is affected by any large anomaly the derivative will deviate from the MTR stabilization described above. Once LTR begins, a downward trend in the derivative suggests an increase in hydraulic diffusivity ( $\eta = 2.64E-4k/\phi\mu c_i$ ) or formation thickness or the presence of pressure support, while an upward trend suggests a decrease in hydraulic diffusivity or formation thickness or the presence of a no-flow boundary(s). Supplementary information should be used when available before drawing conclusions about LTR responses and their causes.

### **Transitions**

Fluid flow in porous media requires transition regions between pressure responses being dominated by various ETR/MTR/LTR effects. From a practical standpoint however, all data prior to MTR are generally considered ETR, and data that deviate from MTR are considered LTR. All regions are not necessarily seen on all tests. It is possible to have ETR and LTR with no recognizable MTR; or to have ETR only. A region that is seen during a test will be in logical order relative to other identifiable regions so that, for example, if LTR is seen it will not precede MTR. What regions are seen during any particular test is dependent upon the duration of ETR effects, test time, and proximity of reservoir anomalies.

### **Plots and Plotting Functions**

Derivative log-log plots consist of the following two curves:

- 1.) pressure function vs time function,

## 2.) pressure function derivative vs time function.

The pressure function is often delta pressure ( $\Delta p = |p_t - p_0|$ ) for the test period, but can be another function of pressure such as real gas pseudopressure.<sup>13</sup> The time function is usually delta time ( $\Delta t = t_t - t_0$ ) for the test period but can be another function of time such as equivalent time<sup>14</sup> or pseudotime.<sup>15</sup> The pressure function derivative is calculated using the appropriate pressure function and time function. It is beyond the scope of this paper to delve into reasons for using any particular pressure function or time function, or to describe methods to calculate the derivative. For interested readers, Ref. 5 provides a look at different differentiation algorithms.

The graphs in this paper will be labelled generically as it is the intent of the paper to concentrate on general diagnostics and not plotting functions. Suffice to say however, the choice of an appropriate plotting function can be critical. For discussion purposes the pressure function curve will be referred to as the pressure curve while the pressure function derivative curve will be referred to as the derivative curve.

The theoretical derivative signatures described below are consistent for constant rate drawdown tests, or buildup tests preceded by long, constant rate drawdowns. These signatures would also be seen for constant rate injection tests, or falloff tests preceded by long, constant rate injection. Derivative signatures can be distorted from what is shown here for buildup and falloff tests where production (or injection) time is short.

## COMMON ETR MODELS AND DIAGNOSTICS

### Wellbore Storage and Skin

During wellbore storage the pressure and derivative curves overlay each other along a unit slope (1/1). After storage effects diminish the derivative attains a local maximum value and then rolls down, producing a "hump". The "hump" may be very prominent to less prominent, or possibly nonexistent with the derivative merely rolling over without the local maximum. The more pronounced humps indicate significant positive apparent skin damage; less pronounced humps indicate less significant skin damage to undamaged conditions; and gently rolling derivatives without maximums indicate negative skin or stimulated conditions. Figs. 4a-c present three scenarios with varying skins. Fig. 4a shows wellbore storage and a large positive skin; Fig. 4b shows wellbore storage and no skin; Fig. 4c shows no wellbore storage and stimulated (negative skin) wellbore conditions.

### Hydraulically Fractured Well

A well intercepting an infinite-conductivity fracture (either hydraulically induced or naturally occurring) can produce the derivative log-log behavior shown in Fig. 5a. The pressure and derivative curves track each other along a half-slope (1/2) trace. The 1/2 slope indicates a

formation linear flow to the fracture, perpendicular to the fracture face. Wellbore storage effects may also be seen (Fig. 5b), while a linear fracture skin on the fracture face and wellbore storage may cause the profile in Fig. 5c. Note in Fig. 5c the derivative "hump" resulting from the linear skin. Fig. 6a presents the one-quarter ( $1/4$ ) slope profile produced by both pressure and derivative in the presence of a finite-conductivity fracture. The  $1/4$  slope is the result of bilinear flow occurring simultaneously in the formation and within the fracture. Figs. 6b-c show the distortion possible with the presence of wellbore storage, and with the presence of wellbore storage and linear fracture skin, respectively. Note that for all cases in this section the derivative starts to flatten as the test response becomes influenced by the infinite-acting bulk reservoir beyond the immediate vicinity of the fracture.

### **Partial Penetration**

When a productive interval is not fully penetrated by the drill bit or if only a portion of a productive interval is perforated, the effects of partial penetration may be seen on the test data. Due to the geometric considerations of partial penetration, it is difficult to generalize about any particular derivative signature. Figs. 7a-c present some possible derivative response scenarios for a well in a zone where only a small interval in the middle of the zone has been perforated. Cases shown in Figs. 7a-b have the same vertical to horizontal permeability ratios ( $k_v/k_h$ ), but Fig. 7a has no wellbore storage effects and a small negative skin. Note that the derivative has a nearly flat portion before departing downward (Fig. 7a). This is due to the response being initially controlled by the capacity ( $kh$ ) of the perforated interval. Eventually, the entire pay zone contributes thus causing the downward trend of the derivative toward a new stabilization controlled by the entire pay zone. Fig. 7b reflects storage effects and a portion of the derivative exhibiting a negative half-slope ( $-1/2$ ) indicative of spherical flow. Fig. 7c presents a case where the permeability ratio is larger and the stabilization according to the entire pay has occurred fairly quickly. A generalization that can be made is that the partial penetration effect produces an apparent skin damage which is aggravated by both low  $k_v/k_h$  and penetration ( $h_p/h$ ) ratios.

### **Horizontal Well**

It is even more difficult to generalize about horizontal well derivative responses than those for partial penetration simply because the geometric possibilities are greater in number. Both radial and linear flow profiles are common, and geometric factors govern which flow regimes, if any, are seen on any particular test. An excellent presentation of the factors controlling the development of flow regimes is given by Odeh and Babu.<sup>16</sup> These factors include horizontal well length ( $L$ ), x,y,z-direction permeabilities ( $k_x$ ,  $k_y$ ,  $k_z$ ), and the placement of the well within the pay zone (i.e., centered, off-centered). Fig. 8a shows an initial stabilized derivative (radial flow) and then a transition to a  $1/2$  slope (linear flow) and then another flattening of the derivative as the test response becomes influenced by the infinite-acting bulk reservoir beyond the immediate influence of the horizontal well. The early radial flow is due to the fluid moving towards the well in a vertical plane perpendicular to the axis of the horizontal well. The

controlling "thickness" during the early radial flow is the length of the well. The subsequent linear flow is due to the fluid moving to the well much as it would in the presence of an infinite-conductivity fracture. Fig. 8b shows essentially the same case as Fig. 8a but with wellbore storage effects included. The responses shown here are not necessarily typical, but represent possibilities.

## **COMMON MTR MODELS AND DIAGNOSTICS**

### **Homogeneous Radial Flow**

The derivative profile is stabilized for the often seen case of infinite-acting homogeneous radial flow. Referring back to Figs. 4a-c, all derivatives there are flattening to stabilization after emerging from the wellbore storage and skin effects region. For damaged cases, the derivative approaches the stabilization from above while for stimulated cases the approach is from below. Therefore, note in Figs. 5a-c and 6a-c the hydraulic-fracture case derivatives approach stabilization from below since those cases represent stimulated wells. (The same argument applies to the horizontal well examples in Figs. 8a-b.) Also, the vertical distance between the pressure and derivative curves once stabilization is achieved provides a qualitative indication of skin: the greater the separation, the higher the apparent skin damage. For example, in the partial penetration case in Fig. 7c, note the relatively large separation between pressure and derivative during MTR even though no actual skin damage was included in the simulated data.

On a broader note, any time the derivative stabilizes for a period of time, the qualitative indication is that a homogeneous or "pseudo" homogeneous radial flow reservoir response, either infinite-acting or semi-infinite acting in nature, has developed. A flat derivative is not necessarily solely indicative of infinite-acting homogeneous radial flow. (See single no-flow boundary discussion below.)

### **Two-Porosity Systems**

Naturally fractured reservoirs typically behave as two-porosity flow systems where the matrix rock represents the primary porosity and the fracture network represents the secondary porosity. Two-porosity reservoir models assume that the majority of the reservoir fluid is stored within the primary porosity but only the more conductive fracture network is directly connected to the wellbore. Therefore fluid must move from matrix to fractures to wellbore with no flow allowed from matrix to wellbore. A popular conceptual model of two-porosity systems is that of Warren and Root<sup>17</sup>, and the profiles shown in Figs. 9a-f were generated using this model. Another well-known two-porosity model is that of Kazemi.<sup>18</sup>

The derivative signatures from these systems are fairly distinctive. They consist of, ideally, an initial flattening which corresponds to infinite-acting radial flow in the fracture network, a drop downward into a "trough" or "dip", and finally a return to the stabilization level from below. The final stabilization is at the same level as the initial stabilization (for Warren and Root

model) and represents a total system (fractures + matrix) infinite-acting radial flow response. The depth and location of the "trough" provides qualitative indication about the relative storativity of the fracture network and the degree of matrix/fracture heterogeneity. The deeper the "trough", the less fluid storage capacity the fracture network has relative to the total storage capacity (fractures + matrix). Practically speaking, the later the trough occurs in time, the smaller the ratio of matrix permeability to fracture permeability. Fig. 9a illustrates a case where there is no wellbore storage and the derivative "dip" is noticeable between the beginning and ending stabilized segments. Fig. 9b differs only in that the "dip" occurs earlier in time while Fig. 9c shows how the effects of wellbore storage might partially obscure the initial derivative flattening. Fig. 9d is similar to Figs. 9a-b except the trough is steeper. Wellbore storage has totally obscured the initial flattening of the derivative for the case presented in Fig. 9e.

### **Radial Composite Systems**

A radial composite system consists of two or more concentric regions; each with different hydraulic diffusivities. For a two-region composite system, there exists an inner region of hydraulic diffusivity which exists out to a distance from the well and beyond that, a different hydraulic diffusivity exists. Although the regional diffusivity change may be due to gross differences in porosities or fluid viscosities, a common reason is different absolute permeabilities. Figs. 10a-c present cases where the inner region permeability ( $k_i$ ) is greater than the outer region permeability ( $k_o$ ), while Figs. 10d-f show the reverse situation. Figs. 10a-b show the same situation except wellbore storage is seen on Fig. 10b. A larger  $k_i/k_o$  ratio is responsible for the steeply rising derivative in Fig. 10c. Fig. 10d presents a case where  $k_i$  is less than  $k_o$ . In Fig. 10e the  $k_i/k_o$  ratio is less than in Fig. 10d. Fig. 10f presents the added effects of wellbore storage. Although composite systems can exist naturally, they may result from intervention, i.e., a greater inner diffusivity may result from a large acid treatment and a lesser inner diffusivity may be the result of deep fluid invasion during drilling. The derivative will stabilize initially corresponding to the influence of the inner diffusivity while later it will restabilize corresponding to the control of the outer diffusivity.

## **COMMON LTR MODELS AND DIAGNOSTICS**

### **Single No-Flow Boundary**

Given enough test time, the derivative may indicate the presence of a no-flow boundary such as a sealing fault. This type of anomaly causes the derivative to depart upward from the MTR stabilization and gradually restabilize at twice the value of the MTR stabilization, which corresponds to the classic slope-doubling behavior seen on the semilog plot. (Should the derivative rise to a level greater than twice the MTR value, suspect multiple no-flow boundaries.) Once the derivative restabilizes, the response is said to be semi-infinite acting and that although a no-flow boundary exists, the reservoir is still open and infinite-acting in all other lateral directions. Figs. 11a-b show the derivative signature for a single no-flow boundary without storage and with storage, respectively. It is not always clear whether a derivative

stabilization is indicating an infinite-acting pressure response or a semi-infinite acting pressure response. Obviously, it is easier to make the call if the MTR stabilization is not obscured by ETR effects.

### **Single Constant-Pressure Boundary**

The effects of a constant pressure source such as an edgewater drive is to arrest the pressure drop during a test, thus causing the derivative to depart downward from the MTR stabilization. Figs. 12a-b show the effects on the derivative in the presence of a constant pressure source without wellbore storage and with storage, respectively. Strong water drives can wash out the effects of no-flow boundaries.

### **Channel Boundaries (Parallel)**

Wells drilled into channel sands may produce the LTR effect of two parallel boundaries. The ideal cases presented in Figs. 13a-b are for a well situated equidistant from the two no-flow boundaries. The upward departure of the derivative from MTR stabilization is of course due to the boundaries; however, notice the pressure and derivative curves track each other along a  $1/2$  slope. This reflects the linear flow to the well as fluid is moving primarily to the well from the long dimensions of the reservoir (parallel to the boundary planes). Note that the LTR derivative rises to a level greater than twice the MTR derivative level.

### **Closed System**

Given enough time, a well test will eventually investigate the limits of the contributory pore volume. Specifically, a closed system is synonymous with volumetric reservoir whereby there is no pressure support and the reservoir is essentially a closed tank. Four theoretical responses are shown here for the case of a well situated in the center of a closed square. Figs. 14a-b present sample drawdown responses. Both the pressure and derivative attain unit slope (a late-time unit slope as opposed to the early time unit slope exhibited by wellbore storage) once the limits of the reservoir have been seen. This behavior occurs when all reservoir no-flow limits are influencing the pressure response and the reservoir is in depletion. Figs. 14c-d present sample buildup responses following a long drawdown during which the reservoir experienced depletion. Note that the derivative drops down rapidly once all limits are seen during the buildup. This results from the pressure rolling over to an average value within the well's contributing pore volume. The closed-system scenario represents an instance where the derivative behavior for drawdown and buildup are distinctly different.

## **TEST DIAGNOSIS HINTS AND EXAMPLES**

Even though real well test data seldom resemble the theoretical responses presented thus far, it is helpful to be familiar with the theoretical responses. To make a systematic diagnosis of a well test based on the derivative log-log plot, the following steps should serve as a guide:



1. Remember that ETR, MTR, and LTR effects should occur in logical order.
2. Keep in mind known information about the well which may influence the ETR behavior. Was the well completed without a packer? If the test is a buildup or falloff test, was the well closed-in at surface or downhole? Is the well horizontal? Has the well been hydraulically fractured or otherwise stimulated? Was the well partially completed to avoid coning water or gas?
3. Keep in mind known information about the reservoir which may influence the MTR behavior. Is the reservoir fairly homogeneous? Are there any expected gross changes in permeability or thickness or possible encounters with a fluid bank? Is a two-porosity system a possibility?
4. Keep in mind known information about boundaries which may influence the LTR behavior. Has a fault been mapped near the well location? Was the well drilled into a channel sand? Is there a strong possibility of a natural water drive? Is there a large gas cap overlying an intended test in an oil zone?
5. With as much knowledge as possible gained a review of possible influencing factors per items 2-4 above, mentally break the test response down into its constituent ETR, MTR, and LTR components (as they apply) and note recognizable pressure and derivative curve slopes and general derivative trends (increasing, decreasing, etc.). Realize that vastly different well/reservoir/boundary models may produce very similar well test responses and if not much is known about a particular formation or area, then it is best to resort to the simplest possible interpretation until additional information becomes available.

The above steps may appear simplistic; however, they represent the piecewise approach necessary to develop a consistent qualitative interpretation. Some actual test responses now follow which show certain combinations of the above described ETR/MTR/LTR models.

### **Case 1: (Fig. 15)**

The early time unit slope behavior of both pressure and derivative curves indicate existence of wellbore storage. After storage the derivative rolls over and down, commensurate with considerable positive skin damage. This buildup test provides no information regarding MTR or LTR.

### **Case 2: (Fig. 16)**

Early unit slope response indicates wellbore storage. The derivative achieves a maximum and proceeds to drop off rapidly. It is believed that rapid drop of the derivative was due to pressure

returning to a static value during the buildup test. Therefore, test shows ETR and LTR effects but MTR has been masked.

### **Case 3: (Fig. 17)**

These pressure buildup data show wellbore storage ETR effect with no MTR stabilization. The cause for the derivative spiking downward is not known. The well was believed to be situated in an isolated channel. LTR shows 1/2 slope behavior on both pressure and derivative curves which supports the channel theory.

### **Case 4: (Fig. 18)**

Test reveals no ETR effects. There is a period of derivative stabilization indicative of infinite-acting radial flow for MTR. Derivative drop-off at end of this falloff test was believed to be due to the LTR effect of a constant pressure source.

### **Case 5: (Fig. 19)**

This falloff test shows 1/2 slope trends on both pressure and derivative curves, indicative of the ETR effects of an infinite-conductivity fracture. The derivative is starting to roll over to a possible stabilization (pseudo-radial MTR behavior) at the end of the test.

### **Case 6: (Fig. 20)**

This falloff test shows 1/4 slope trends on both pressure and derivative curves, indicative of a finite-conductivity fracture. The derivative is starting to roll over to a possible MTR stabilization at the end of the test.

### **Case 7: (Fig. 21)**

This horizontal well buildup test shows wellbore storage and skin and a subtle dip at the end of the test which is believed to be due to two-porosity behavior. Test does not show any LTR effects.

### **Case 8: (Fig. 22)**

This horizontal well buildup test reveals no wellbore storage. There appears to be an initial early derivative stabilization (early radial flow). As in case 7, there is a dip in the derivative (two-porosity behavior), and then a final rise. The well was believed to be situated relatively close to a no-flow boundary(s) in a known two-porosity system.

### **Case 9: (Fig. 23)**

This falloff test shows wellbore storage effects early with a derivative rollover to stabilization. The initial flattening was believed to be due to the MTR effects of an inner region diffusivity in a two-region radial composite system. The subsequent derivative rise was due to the transitional influence of the decreased hydraulic diffusivity of the outer region. The derivative did not restabilize but dropped off at the end of the test. It is believed that the pressure was approaching a static level at the end of the test and prevented a final MTR stabilization due to the outer region.

### **CONCLUSIONS**

Derivative diagnostics presented in this paper should allow the casual student of well test analysis to become familiar with some frequently seen test responses. Well testing and well test analysis are important and beneficial tools in characterizing reservoir behavior and predicting performance. Corroborating information should be utilized to the extent possible when analyzing well test data. Finally, when in doubt about either a qualitative well test interpretation or a quantitative well test analysis, seek the advice of an expert.

## NOMENCLATURE

$c_t$	=	Total system compressibility, $\text{psi}^{-1}$
$h$	=	Formation thickness, ft
$h_p$	=	Perforated interval, ft
$k$	=	Absolute permeability, md
$k_h$	=	Horizontal permeability, md
$k_i$	=	Inner region permeability, md
$k_o$	=	Outer region permeability, md
$k_v$	=	Vertical permeability, md
$k_x$	=	X-direction permeability, md
$k_y$	=	Y-direction permeability, md
$k_z$	=	Z-direction permeability, md
$L$	=	Horizontal well length, ft
$p$	=	Pressure, psi
$p_0$	=	Pressure at start of test period, psi ( $\Delta t=0$ )
$p_t$	=	Recorded pressure during test period, psi
$t$	=	Time, hrs
$t_0$	=	Time at start of test period, hrs ( $\Delta p=0$ )
$t_t$	=	Recorded time during test period, hrs

### Greek Symbols

$\Delta$	=	Difference
$\eta$	=	Hydraulic diffusivity, $\text{ft}^2/\text{hr}$
$\mu$	=	Viscosity, cp
$\phi$	=	Effective porosity, fraction

## REFERENCES

1. Tiab, D. and Kumar, A.: "Application of the  $p_D$  Function to Interference Analysis," JPT (Aug. 1980) 1465-70.
2. Tiab, D. and Kumar, A.: "Detection and Location of Two Parallel Sealing Faults Around a Well," JPT (Oct. 1980) 1701-08.
3. Tiab, D. and Puthigai, S.K.: "Pressure-Derivative Type Curves for Vertically Fractured Wells," SPEFE (Mar. 1988) 156-158.
4. Bourdet, D., Whittle, T.M., Douglas, A.A., and Pirard, Y.M.: "A New Set of Type Curves Simplifies Well Test Analysis," World Oil (May 1983) 95-106.
5. Bourdet, D., Ayoub, J.A., and Pirard, Y.M.: "Use of Pressure Derivative in Well-Test Interpretation," SPEFE (Jun. 1989) 293-302.
6. Bourdet, D., Ayoub, J.A., Whittle, T.M., Pirard, Y.M., and Kniazeff, V.: "Interpreting Well Tests in Fractured Reservoirs," World Oil (Oct. 1983) 77-87.
7. Bourdet, D., Alagoa, A., Ayoub, J.A., and Pirard, Y.M.: "New Type Curves Aid Analysis of Fissured Zone Well Tests," World Oil (Apr. 1984) 111-24.
8. Agarwal, R.G., Al-Hussainy, R., and Ramey, H.J. Jr.: "An Investigation of Wellbore Storage and Skin Effect in Unsteady Liquid Flow: I. Analytical Treatment," SPEJ (Sept. 1970) 279-90.
9. Gringarten, A.C., Bourdet, D.P., Landel, P.A., and Kniazeff, V.J.: "A Comparison Between Different Skin and Wellbore Storage Type-Curves for Early-Time Transient Analysis," paper SPE 8205 presented at the 1979 SPE Annual Technical Conference and Exhibition, Las Vegas, NV, Sept. 23-26.
10. Ehlig-Economides, C.: "Use of the Pressure Derivative for Diagnosing Pressure-Transient Behavior," JPT (Oct. 1988) 1280-1282.
11. Koederitz, L.F.: Notes on Well Test Analysis, University of Missouri-Rolla (July 1985).
12. Lee, John: Well Testing, Textbook Series, SPE, Richardson, TX (1982).
13. Al-Hussainy, R., and Ramey, H.J. Jr.: "Application of Real Gas Flow Theory to Well Testing and Deliverability Forecasting," JPT (May 1966) 637-642.
14. Agarwal, R.G.: "A New Method to Account for Producing Time Effects When Drawdown Type Curves are Used to Analyze Pressure Buildup and Other Test Data," paper SPE 9289 presented at the 1980 SPE Annual Technical Conference and Exhibition, Dallas, TX, Sept. 21-24.
15. Agarwal, R.G.: "Real Gas Pseudotime - A New Function for Pressure Buildup Analysis of Gas Wells," paper SPE 8279 presented at the 1979 SPE Annual Technical Conference and Exhibition, Las Vegas, NV, Sept. 23-26.
16. Odeh, A.S., and Babu, D.K.: "Transient Flow Behavior of Horizontal Wells: Pressure Drawdown and Buildup Analysis," SPEFE (Mar. 1990) 7-15.
17. Warren, J.E., and Root, P.J.: "The Behavior of Naturally Fractured Reservoirs," SPEJ (Sept. 1963) 245-255.
18. Kazemi, H.: "Pressure Transient Analysis of Naturally Fractured Reservoirs With Uniform Fracture Distribution," SPEJ (Dec. 1969) 451-462.

## ACKNOWLEDGEMENTS

The author thanks the management of Halliburton Energy Services for permission to publish this paper. Particular thanks go to Mohamed Soliman and James Hunt for critiquing the paper, and to Rayleene Morris for assistance in producing the paper.

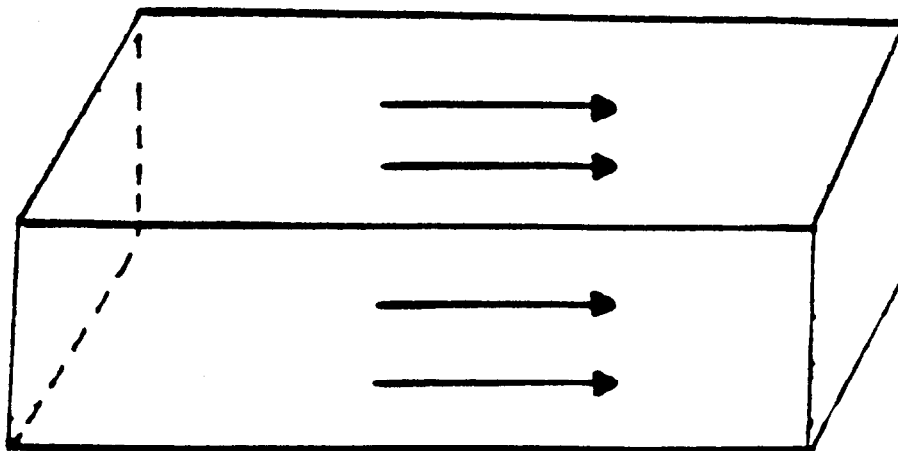


Figure 1 - Linear flow schematic (After Koederitz<sup>11</sup>)

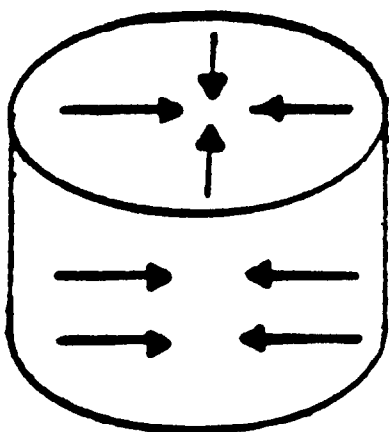


Figure 2 - Radial flow schematic (After Koederitz<sup>11</sup>)

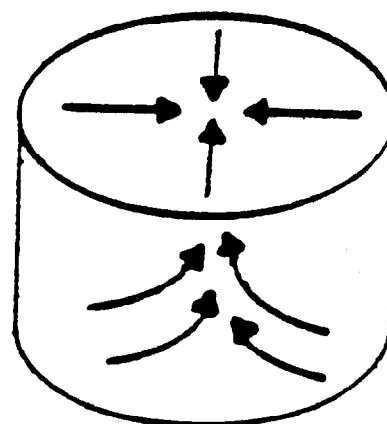


Figure 3 - Spherical flow schematic (After Koederitz<sup>11</sup>)

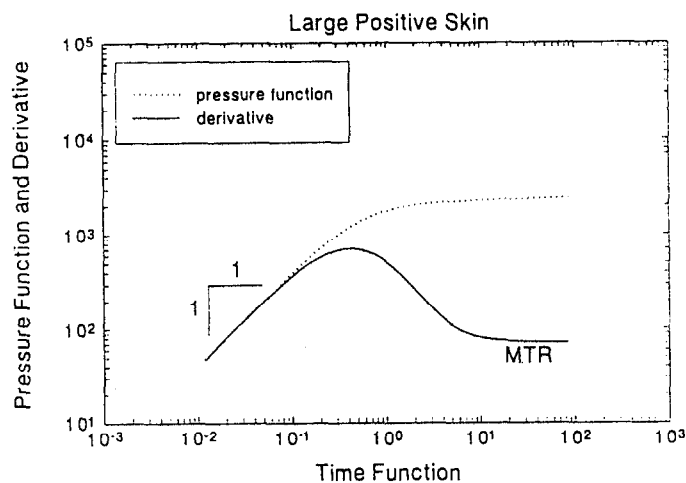


Figure 4a - Wellbore storage and skin

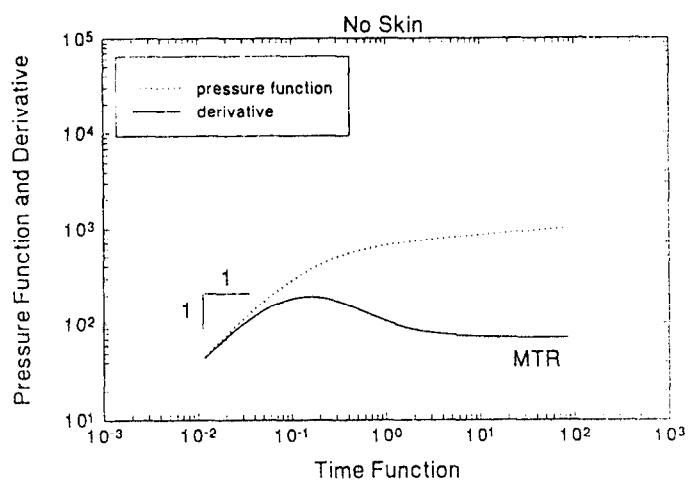


Figure 4b - Wellbore storage and skin

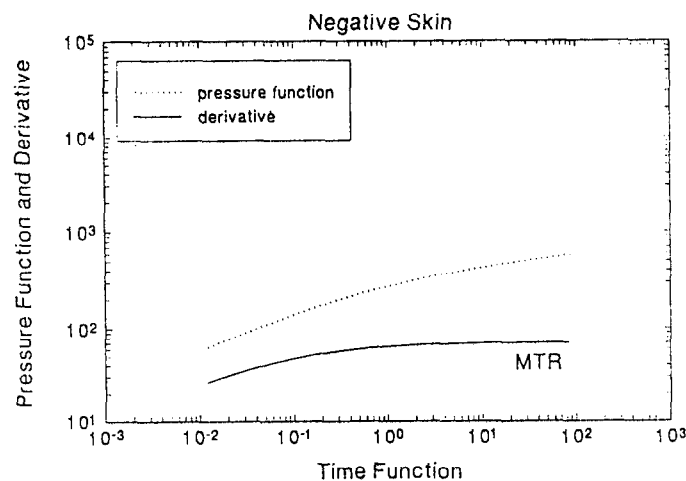


Figure 4c - Wellbore storage and skin

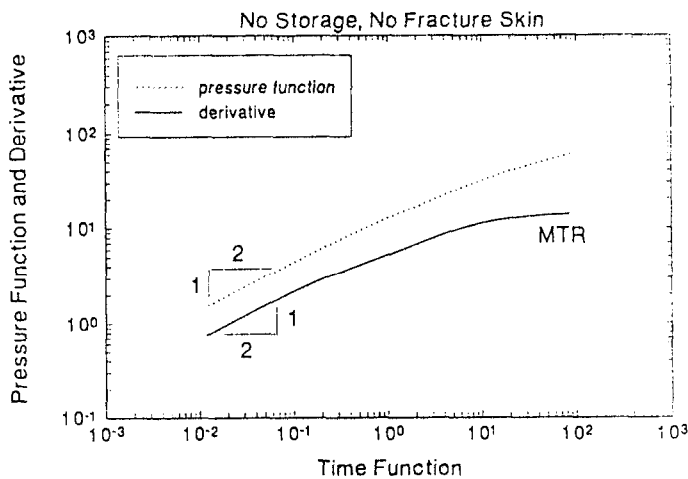


Figure 5a - Infinite conductivity fracture

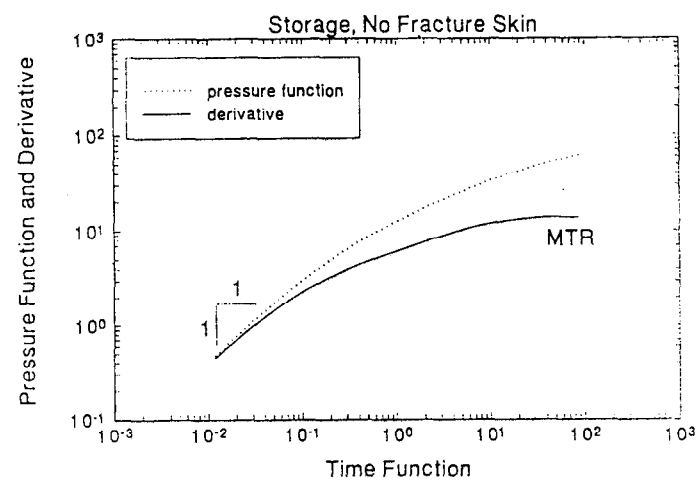


Figure 5b - Infinite conductivity fracture

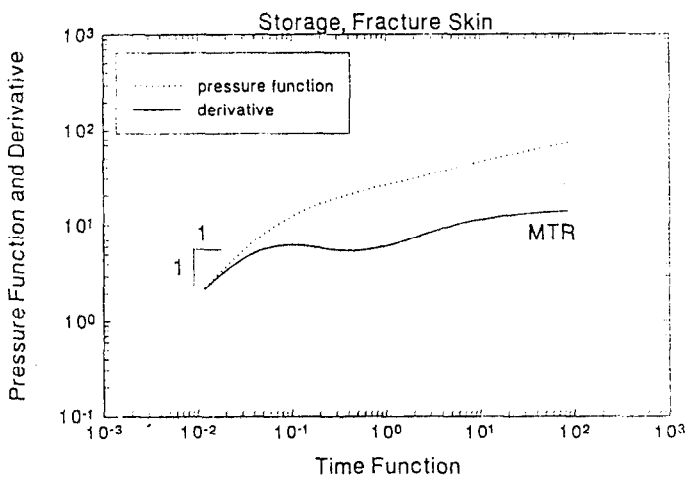


Figure 5c - Infinite conductivity fracture

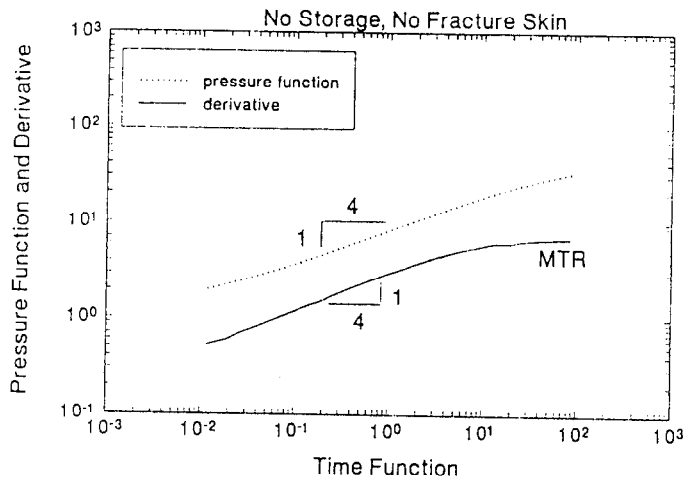


Figure 6a - Finite conductivity fracture

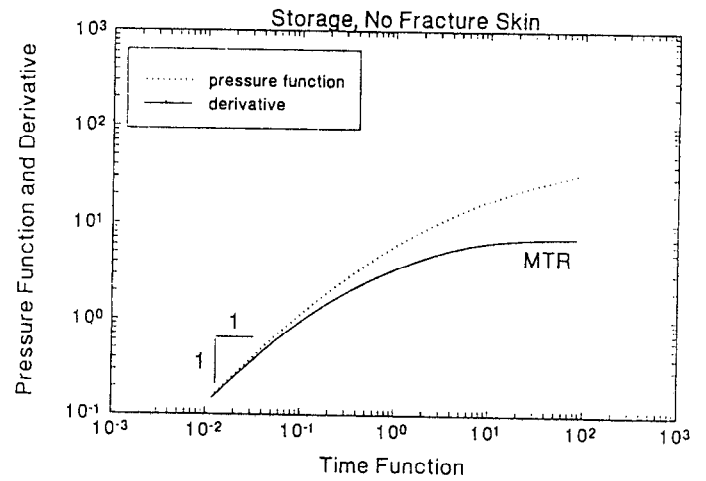


Figure 6b - Finite conductivity fracture

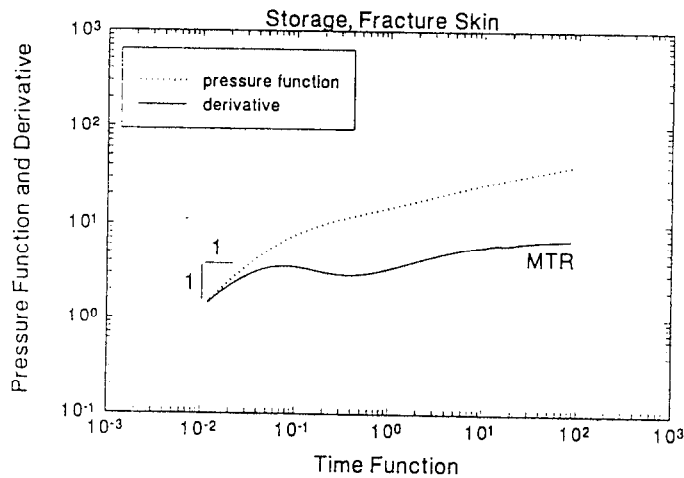


Figure 6c - Finite conductivity fracture

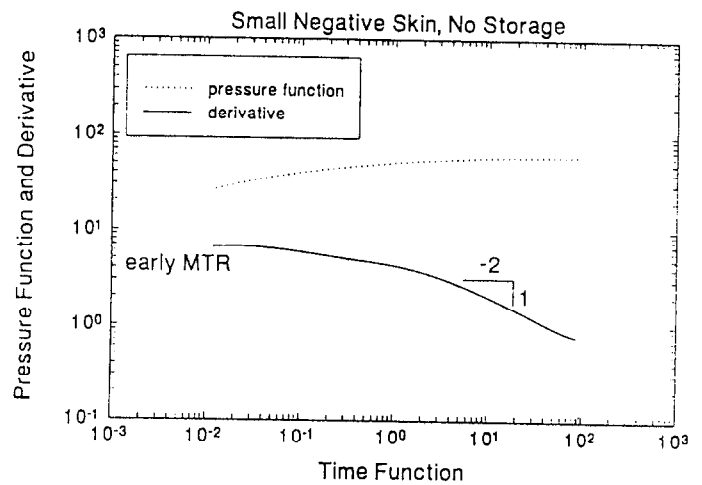


Figure 7a - Partial penetration

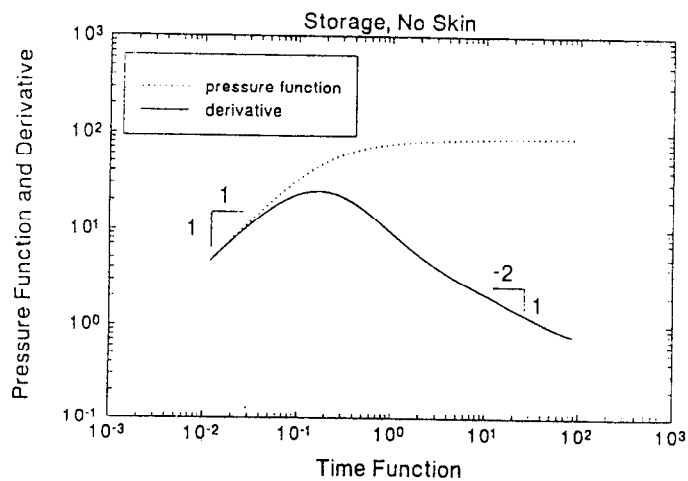


Figure 7b - Partial penetration

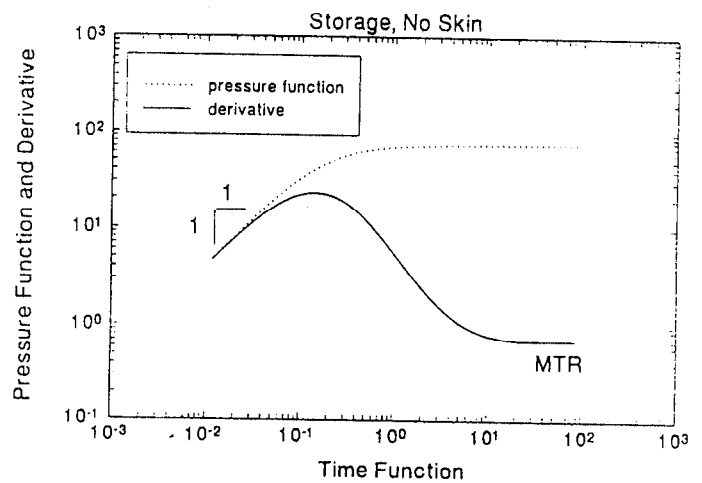


Figure 7c - Partial penetration



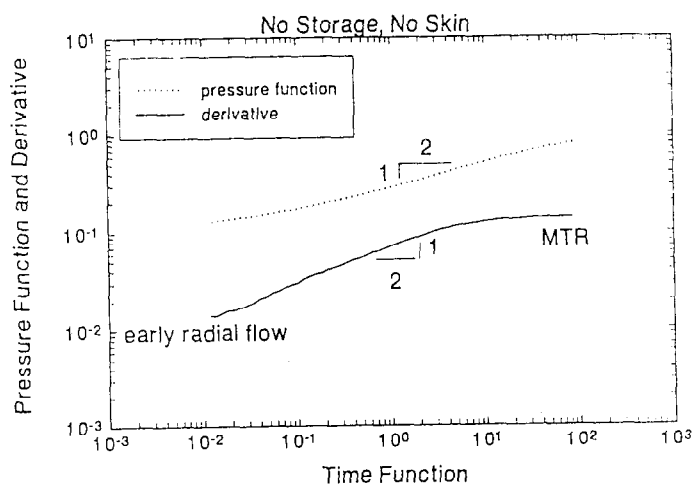


Figure 8a - Horizontal well

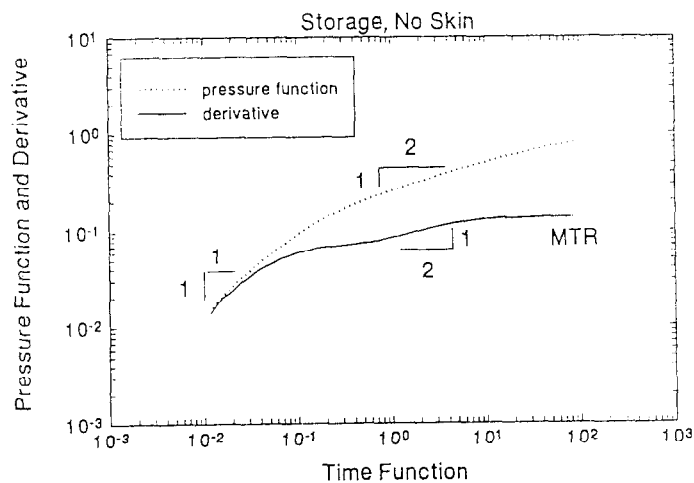


Figure 8b - Horizontal well

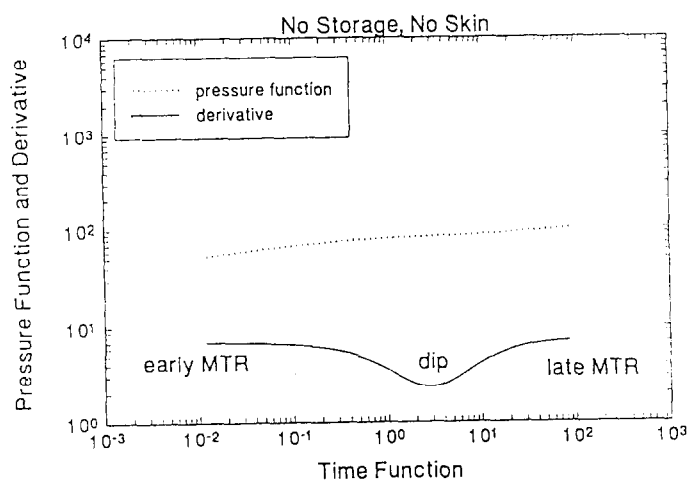


Figure 9a - Two porosity

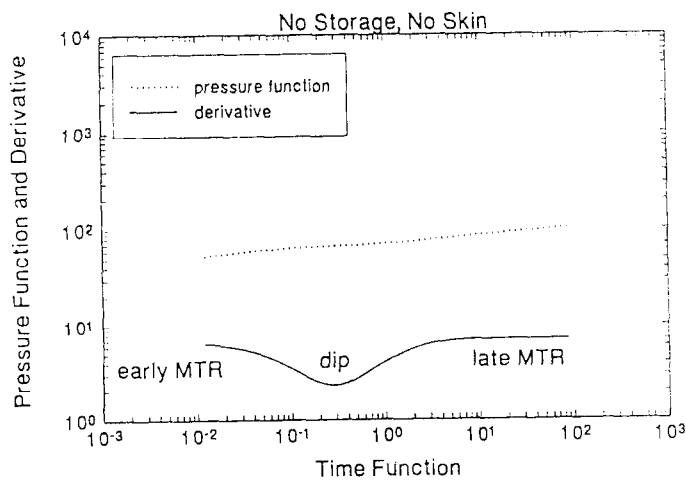


Figure 9b - Two porosity

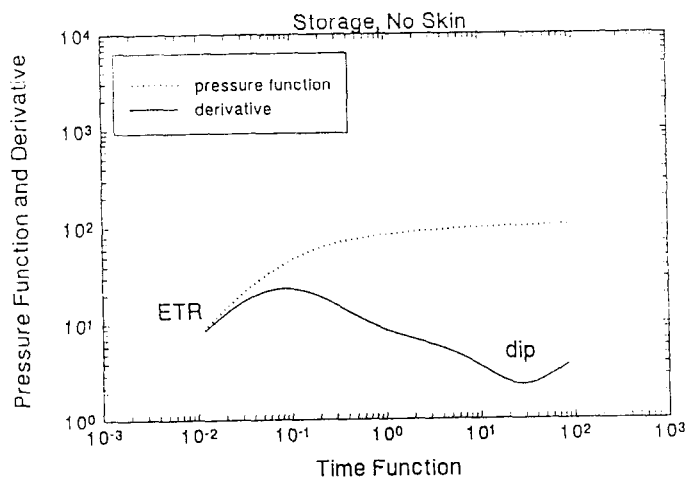


Figure 9c - Two porosity

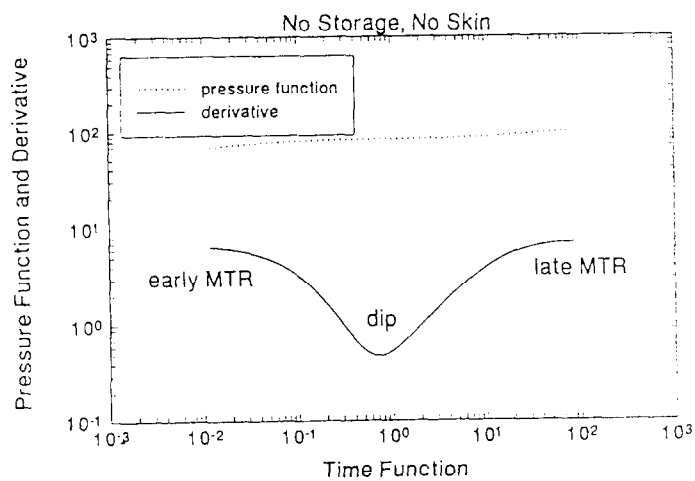


Figure 9d - Two porosity

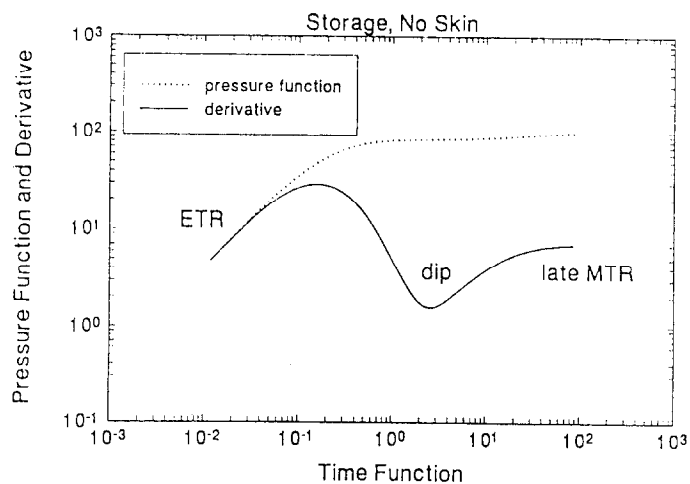


Figure 9e - Two porosity

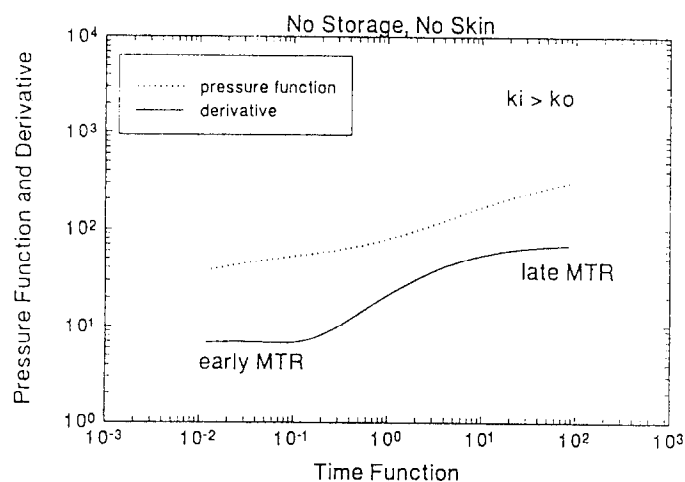


Figure 10a - Radial composite

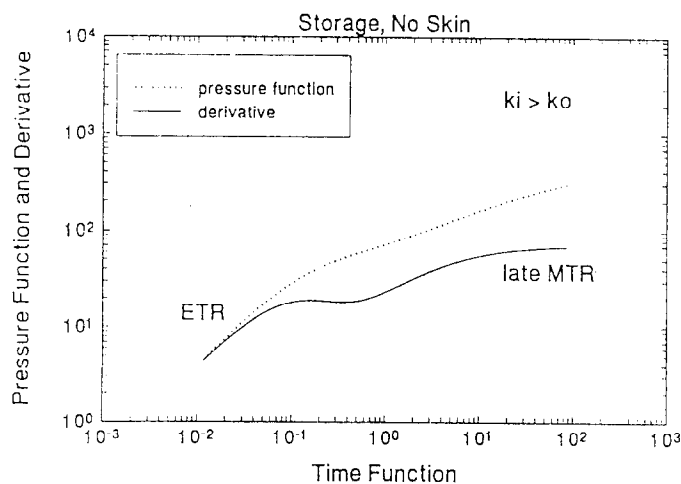


Figure 10b - Radial composite

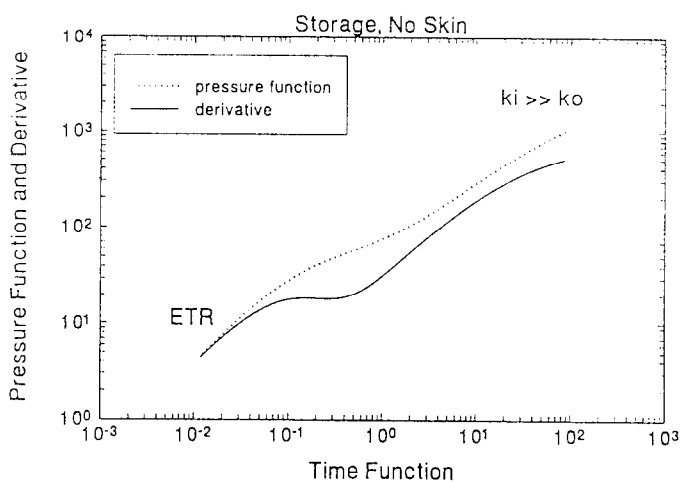


Figure 10c - Radial composite

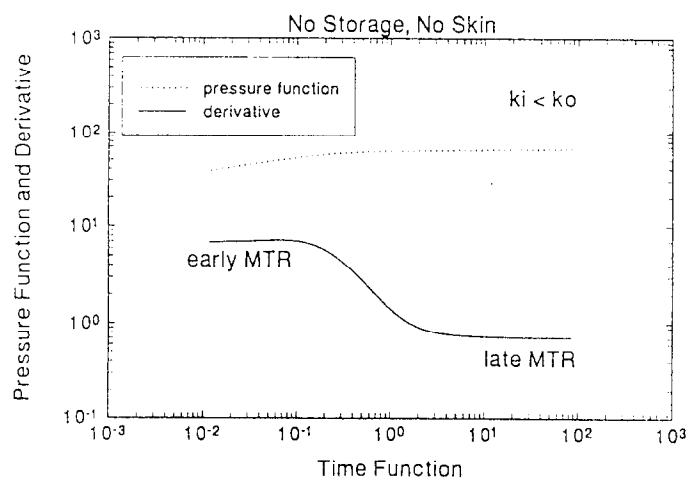


Figure 10d - Radial composite

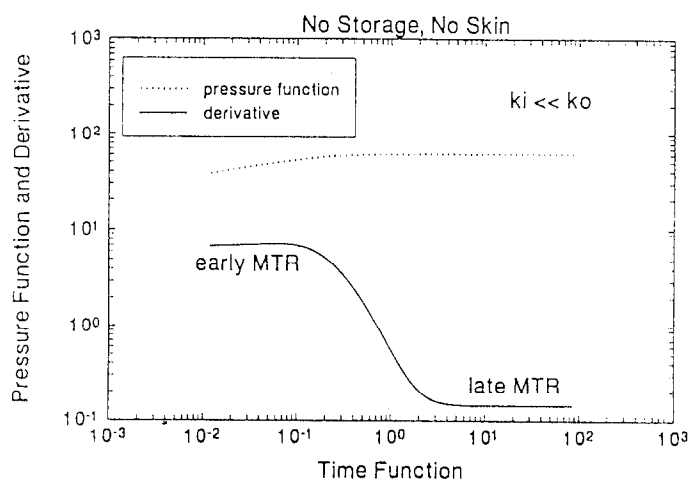


Figure 10e - Radial composite

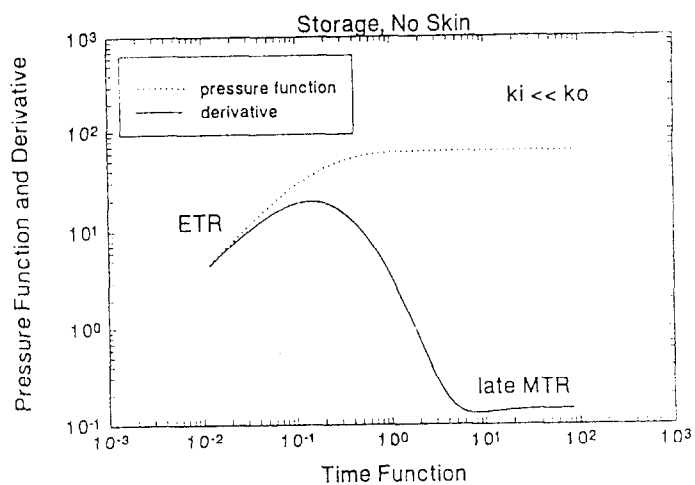


Figure 10f - Radial composite

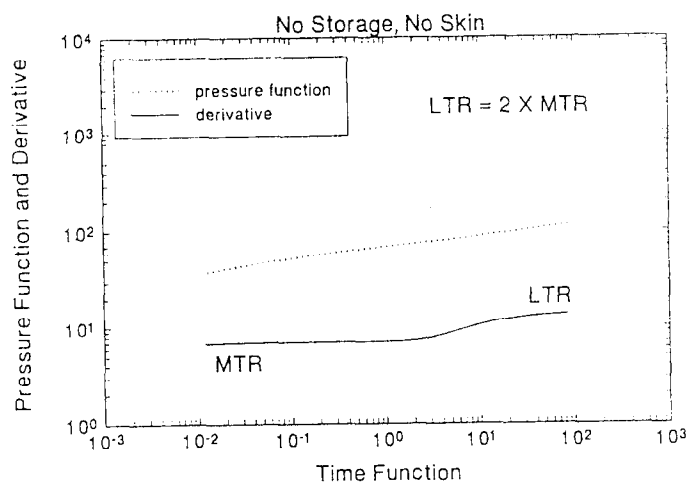


Figure 11a - No-flow boundary

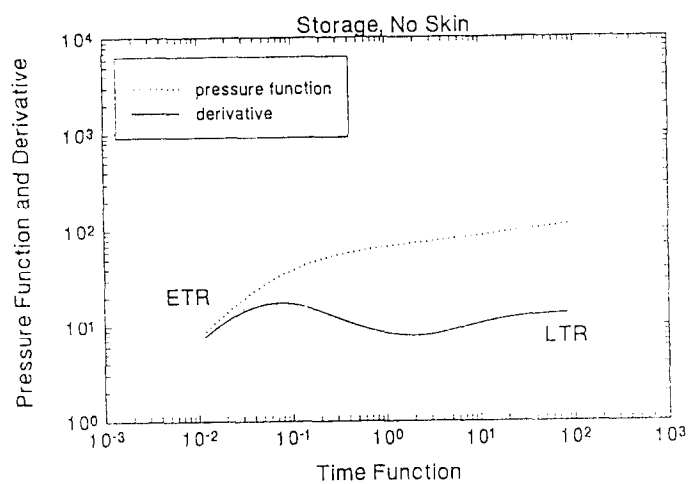


Figure 11b - No-flow boundary

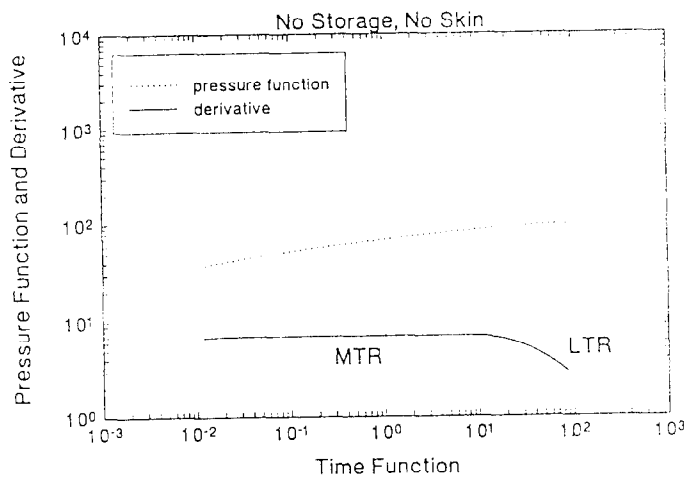


Figure 12a - Constant pressure boundary

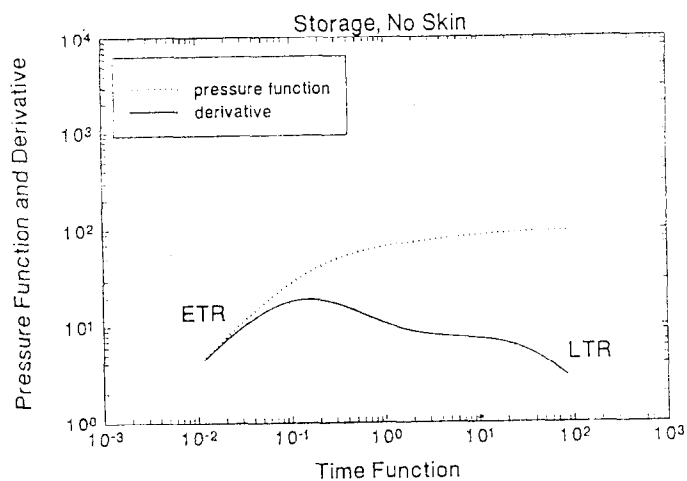


Figure 12b - Constant pressure boundary

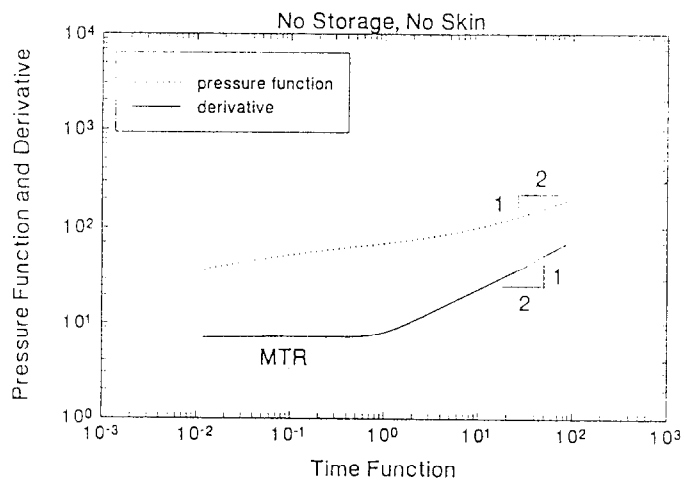


Figure 13a - Parallel boundaries

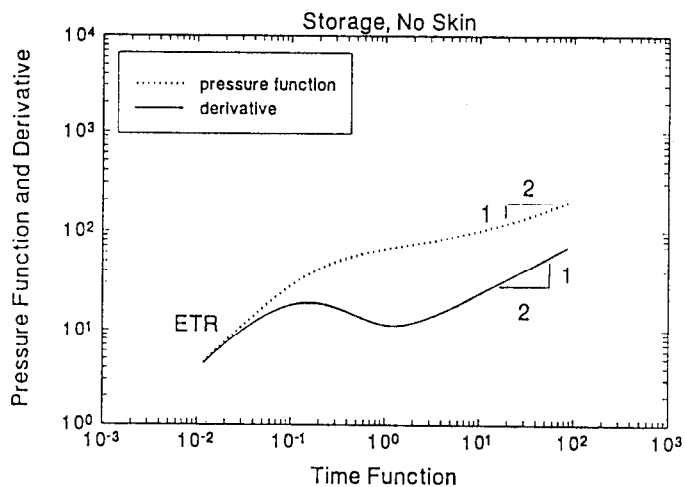


Figure 13b - Parallel boundaries

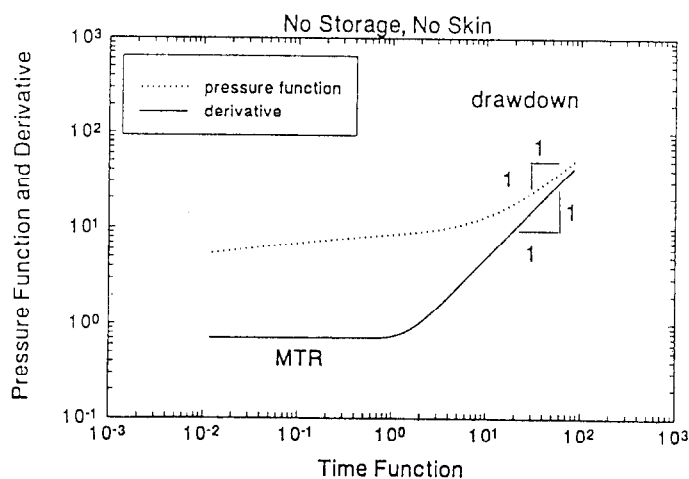


Figure 14a - Closed system/square

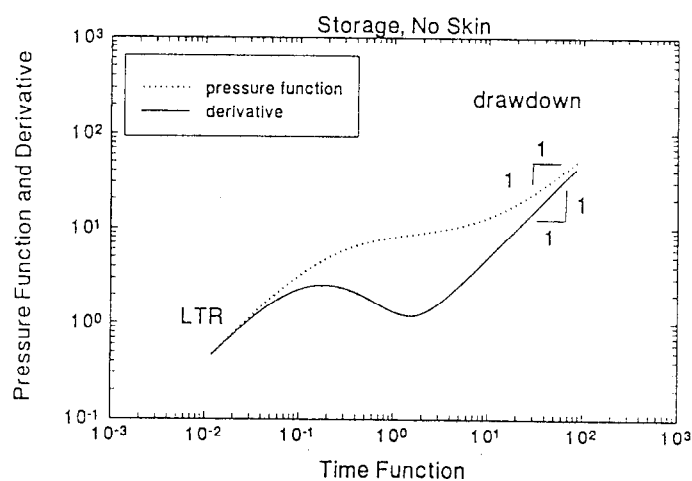


Figure 14b - Closed system/square

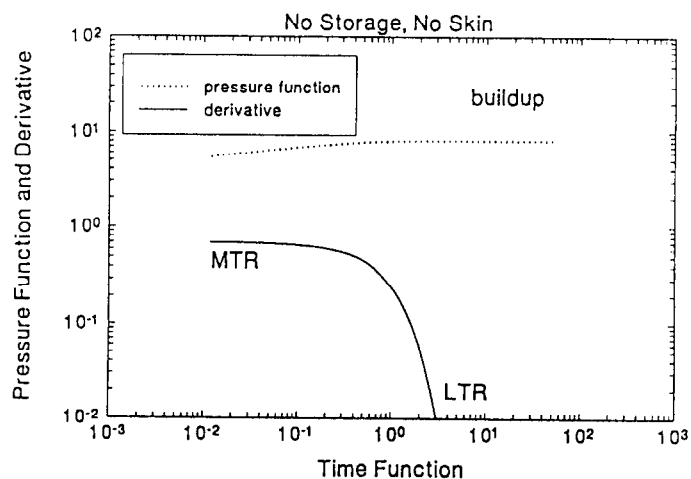


Figure 14c - Closed system/square

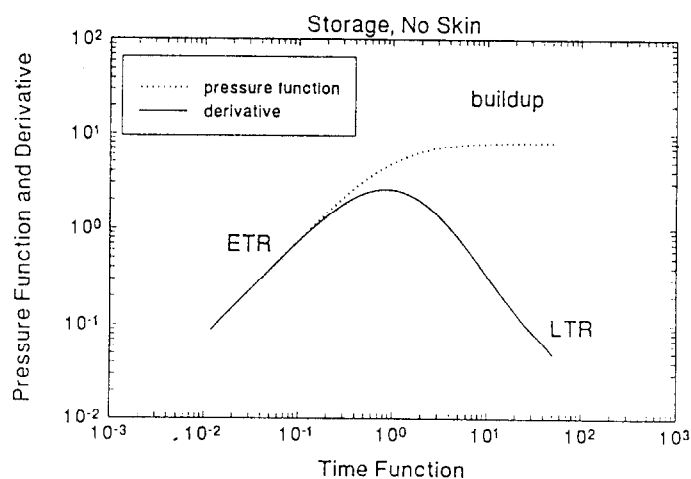


Figure 14d - Closed system/square

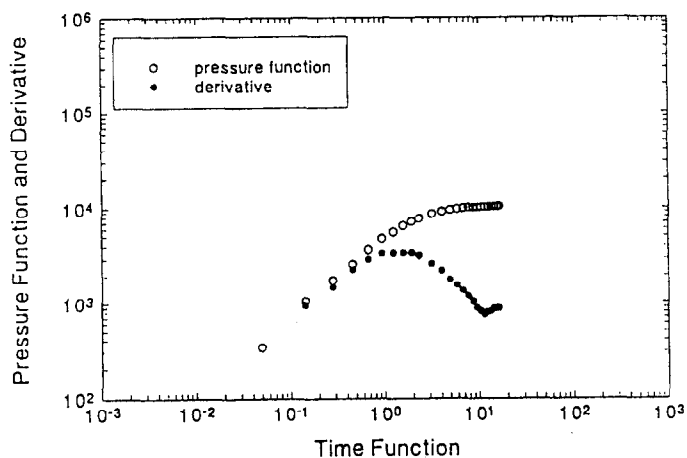


Figure 15 - Case 1 derivative log-log plot

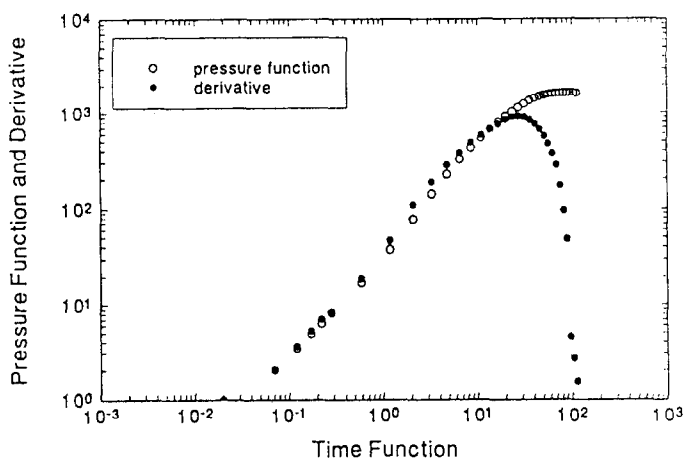


Figure 16 - Case 2 derivative log-log plot

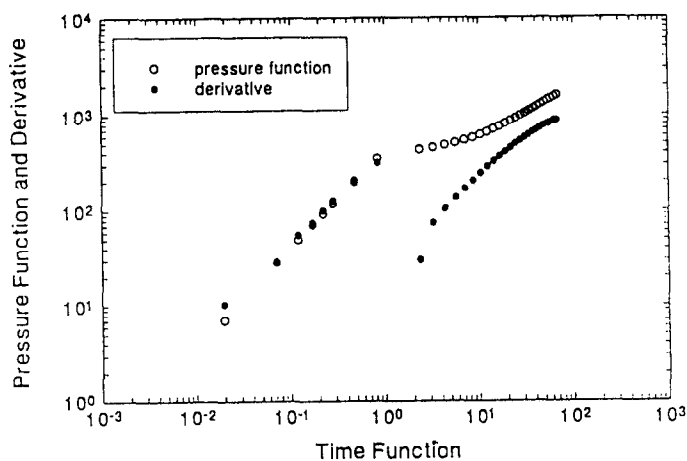


Figure 17 - Case 3 derivative log-log plot

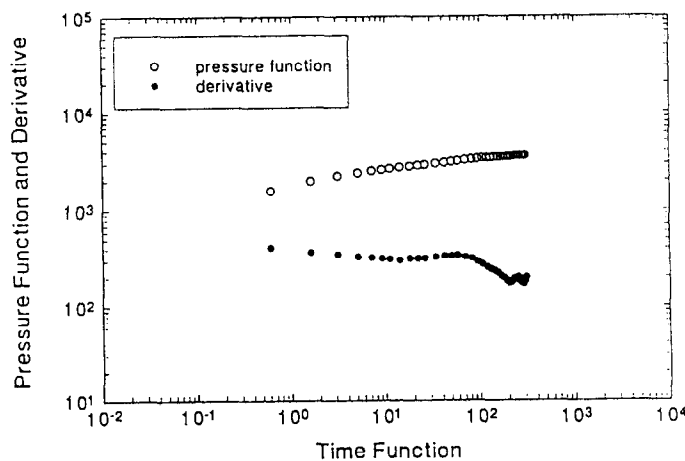


Figure 18 - Case 4 derivative log-log plot

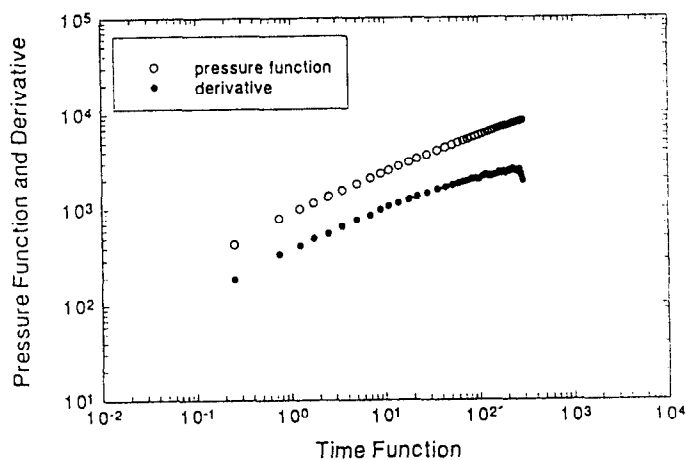


Figure 19 - Case 5 derivative log-log plot

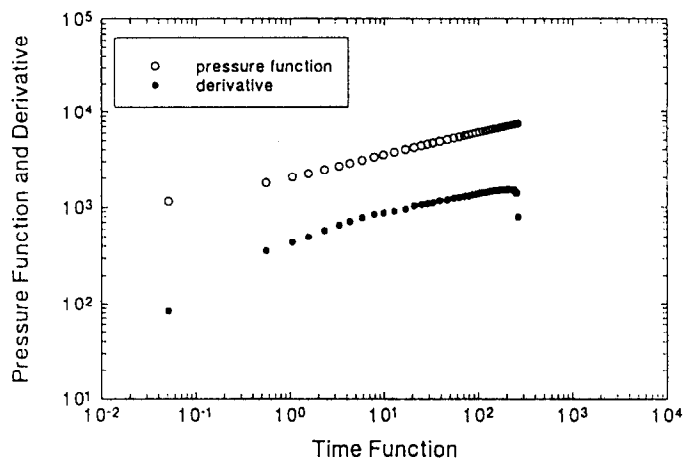


Figure 20 - Case 6 derivative log-log plot

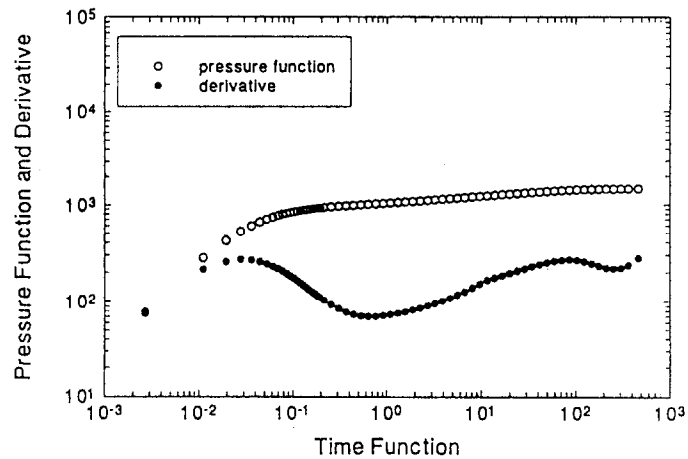


Figure 21 - Case 7 derivative log-log plot

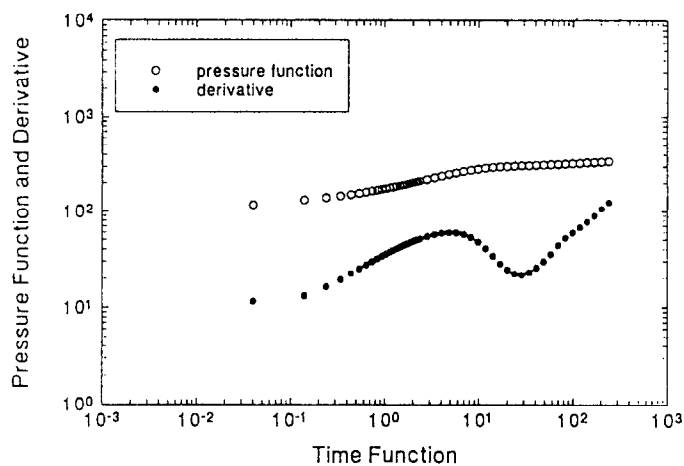


Figure 22 - Case 8 derivative log-log plot

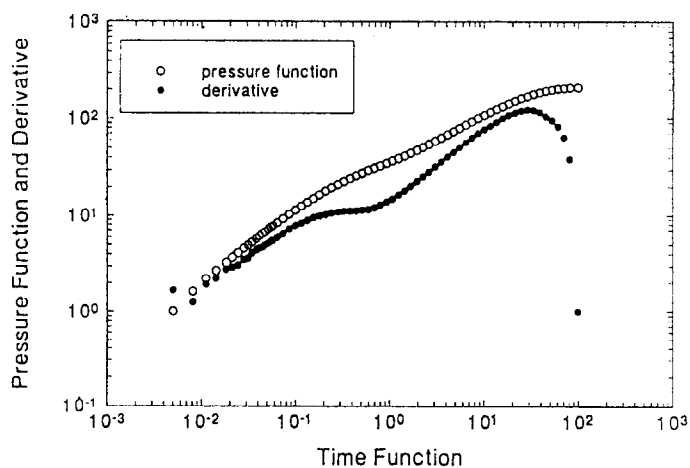


Figure 23 - Case 9 derivative log-log plot